BIOCHEMISTRY
including biophysical chemistry & molecular biology

Article

pubs.acs.org/biochemistry

Structural and Mechanistic Insights into the PAPS-Independent Sulfotransfer Catalyzed by Bacterial Aryl Sulfotransferase and the Role of the DsbL/DsbI System in Its Folding

Goran Malojčić,*[,†] Robin L. Owen,[‡] and Rudi Glockshuber[†]

[†]Institute of Molecular Biology and Biophysics, ETH Zurich, CH-8093 Zurich, Switzerland

[‡]Diamond Light Source, Harwell Science and Innovation Campus, Didcot, Oxfordshire OX11 0DE, U.K.

Supporting Information

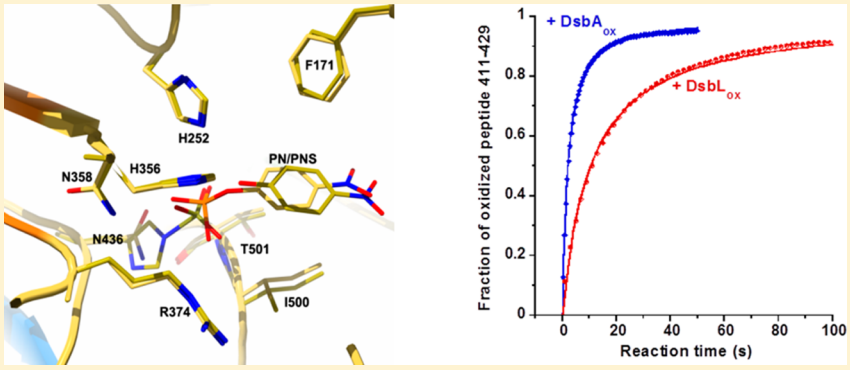

ABSTRACT: Bacterial aryl sulfotransferases (ASSTs) catalyze sulfotransfer from a phenolic sulfate to a phenol. These enzymes are frequently found in pathogens and upregulated during infection. Their mechanistic understanding is very limited, and their natural substrates are unknown. Here, the crystal structures of *Escherichia coli* CFT073 ASST trapped in its presulfurylation state with model donor substrates bound in the active site are reported, which reveal the molecular interactions governing substrate recognition. Furthermore, spectroscopic titrations with donor substrates and sulfurylation kinetics of ASST illustrate that this enzyme binds substrates in a 1:1 stoichiometry and that the active sites of the ASST homooligomer act independently. Mass spectrometry and crystallographic experiments of ASST incubated with human urine demonstrate that urine contains a sulfuryl donor substrate. In addition, we examined the capability of the two paralogous dithiol oxidases present in uropathogenic *E. coli* CFT073, DsbA, and the ASST-specific enzyme DsbL, to introduce the single, conserved disulfide bond into ASST. We show that DsbA and DsbL introduce the disulfide bond into unfolded ASST at similar rates. Hence, a chaperone effect of DsbL, not present in DsbA, appears to be responsible for the dependence of efficient ASST folding on DsbL *in vivo*. The conservation of paralogous dithiol oxidases with different substrate specificities in certain bacterial strains may therefore be a consequence of the complex folding pathways of their substrate proteins.

Sulfotransferases (STs) are enzymes that catalyze the transfer of a sulfuryl group from a donor to an acceptor substrate. Their physiological roles include hormone regulation, detoxification of toxic compounds, and metabolism of xenobiotics. Sulfurylation is regarded as an extracellular signaling mechanism similar to phosphorylation inside the cell.[1]

On the basis of their specificity toward the sulfuryl donor compound, STs can be divided into two groups: those that transfer sulfuryl from 3′-phosphoadenosine-5′-phosphosulfate (PAPS) define a well-studied class of STs, termed PAPS-dependent ST.[1] However, a different class of STs exists that transfer sulfuryl groups from a phenolic ester to a phenol and are termed arylsulfate sulfotransferases, or aryl sulfotransferases, or ASSTs (Scheme 1).

In contrast to PAPS-dependent ST, little is known about ASSTs. ASSTs are present in a number of bacterial organisms,[2−5] especially pathogens,[6] and are linked to virulence.[6−8] Among *E. coli* strains, they are present only in those that cause urinary tract infections, and ASST levels are upregulated during infection.[9] In addition, ASST-like proteins have recently been found to take part in the biosynthesis of liponucleoside antibiotics in *Streptomycetes*.[10−13] ASSTs are capable of utilizing a range of phenolic substrates[2,14] and, albeit at a lower efficiency, even nonphenolic substrates.[15] Therefore,

Scheme 1. Sulfotransfer Catalyzed by ASST[a]

$$Ar\text{-}OSO_3^- + Ar'\text{-}OH \xrightarrow{ASST} Ar\text{-}OH + Ar'\text{-}OSO_3^-$$

[a]Ar and Ar′ symbolize aromatic rings.

Received: December 31, 2013
Revised: February 26, 2014
Published: March 6, 2014

Table 1. Crystallographic Data Collection and Refinement Statistics[a]

	ASST-H436N-PNS	ASST-H436N-MUS	ASST-H436N-apo	ASST-urine
		Data Collection		
space group	$P3_212$	$P3_212$	$P3_212$	$P3_212$
cell dimensions				
a (= b), c (Å)	181.0, 99.4	181.5, 100.4	181.5, 99.6	182.3, 101.6
α (= β), γ (deg)	90.00, 120.00	90.00, 120.00	90.00, 120.00	90.00, 120.00
resolution (Å)	52.26−2.05 (2.16−2.05)	52.40−2.10 (2.21−2.10)	51.02−1.95 (1.98−1.95)	48.35−2.59 (2.66−2.59)
R_{merge}	0.069 (0.687)	0.065 (0.740)	0.072 (0.854)	0.103 (0.807)
$I/\sigma(I)$	20.1 (2.8)	13.9 (1.8)	12.8 (1.6)	9.8 (1.7)
completeness (%)	99.9 (100.0)	99.9 (99.9)	91.1 (94.0)	98.2 (91.4)
redundancy	7.5 (7.5)	4.5 (4.5)	6.3 (5.9)	4.8 (4.1)
		Refinement		
resolution (Å)	50.95−2.05	51.13−2.10	51.02−1.95	48.40−2.59
no. reflections	115946	109496	123127	55613
R_{work}/R_{free}	0.188/0.225	0.214/0.236	0.150/0.169	0.191/0.235
r.m.s. deviations				
bond lengths (Å)	0.0227	0.0135	0.0088	0.0239
bond angles (deg)	1.764	1.582	1.116	1.660
B factors				
protein	40.6	45.1	45.5	48.0
ligand	51.2	53.1	57.3	
water	41.9	36.36	49.2	39.1
Ramachandran statistics				
Resi. in favored regions	1077 (96.33%)	1061 (94.90%)	1042 (92.95%)	1072 (94.87%)
Resi. in allowed regions	38 (3.40%)	53 (4.74%)	75 (6.69%)	51 (4.51%)
outliers[b]	3 (0.27%)	4 (0.36%)	4 (0.36%)	7 (0.62%)
MolProbity score	1.77	2.25	2.56	1.84
PDB ID code	4P05	4P06	4P04	4P07

[a]Values in parentheses are for the highest-resolution shell. [b]The outlier residues are at the border of favored regions and are either glycines or forming the active site, and the energy required to distort the preferred conformation is most likely compensated by the energy of ligand binding, as observed in the structure of the wild-type protein.[17]

they may be useful as a green way to perform sulfurylation without the need for functional group protection during organic synthesis.[15]

The structure of ASST from uropathogenic *Escherichia coli* CFT073[16] has recently been reported in the apo-state and after enzyme sulfurylation by the sulfuryl donor, with products of the first half-reaction bound to the active site.[17] This enzyme follows the ping−pong bi−bi kinetic mechanism, where the active site histidine residue undergoes transient sulfurylation of its $N^{\varepsilon 2}$ atom by the sulfuryl donor and subsequently delivers this sulfuryl group to the acceptor.[17]

The absence of an ASST structure with the aryl sulfate donor in the active site has limited our structural understanding of enzyme sulfurylation and the roles conserved active site residues play in catalysis. The rate limiting step and the kinetic parameters of enzyme sulfurylation are also unknown. Furthermore, since half-site reactive STs have been described,[18] it needed to be clarified whether all or only one-half of the active sites of ASST, which crystallized as a homodimer, participate in catalysis at any given time. The natural substrates of ASST are elusive, but since *E. coli* CFT073 is a uropathogen and ASST is upregulated during urinary tract infections, it is likely that it functions in the pathogenic habitat. Therefore, it remained to be determined if human urine contained compound(s) that could act as ASST substrates. In addition, efficient folding of ASST in the periplasm proved to be dependent on the ASST-specific dithiol oxidase DsbL.[19] ASST contains a single structural disulfide bond (Cys418-Cys424) per monomer, which could be introduced by DsbL or the generic dithiol oxidase DsbA.[19] It is unclear whether the dependence of ASST folding on DsbL stems from a fast ASST oxidation by DsbL or is due to a chaperone effect of DsbL. The crystallographic and biochemical work described here addresses these limitations in our understanding of ASSTs and provides novel insights into their reaction mechanism and biogenesis.

MATERIALS AND METHODS

Protein Expression and Purification. ASST amino acid variants were generated, expressed, and purified following the procedures described.[17] DsbL was prepared as described.[19]

Crystallography. ASST(His436Asn) crystals were obtained via the sitting drop vapor diffusion method by equilibrating 1.5 μL of protein solution (22 mg/mL, in 20 mM 4-morpholinepropanesulfonic acid/NaOH at pH 7.5, 100 mM NaCl) with 0.5 μL of reservoir solution consisting of 1.8 M Li_2SO_4 and 100 mM cacodylic acid/NaOH at pH 6.5. Crystals were cryoprotected by dragging them through paraffin oil (Hampton, USA) before flash-cooling in a nitrogen cryostat. X-ray diffraction data were collected at the beamline X06SA at the Swiss Light Source (SLS), at a wavelength of 1.000 Å. Diffraction data were integrated using XDS[20] and scaled using SCALA.[21] Significant crystal twinning was observed, with the twin fraction being 0.442/0.558, 0.59/0.41, and 0.52/0.48 in apo-ASST, 4-nitrophenyl sulfate (PNS)-soaked, and 4-methyl-umbelliferyl sulfate (MUS)-soaked, respectively. Structures were solved by molecular replacement using Phaser[22] and refined using Coot,[23] Refmac,[24] and Phenix[25] (Table 1). Molprobity[26] was used to assess the resulting models.

dx.doi.org/10.1021/bi401725j | *Biochemistry* 2014, 53, 1870−1877

Crystals of catalytic intermediates of ASST were obtained by soaking native crystals of ASST(His436Asn) with a reservoir solution composed of either 1.6 M Li_2SO_4, 88.8 mM cacodylic acid/NaOH at pH 6.5, and 5 mM PNS or 1.44 M Li_2SO_4, 80 mM cacodylic acid/NaOH at pH 6.5, and 5 mM MUS. Crystals of ASST with human urine were obtained by soaking native crystals of ASST with a solution containing 1.2 M Li_2SO_4 and 100 mM cacodylic acid/NaOH at pH 6.5 dissolved in human urine. These solutions were added stepwise and left to equilibrate for 15 min prior to cryo-cooling as described above. X-ray diffraction data were collected at beamline X06SA of the SLS. Initial maps and models of catalytic intermediates were obtained by refinement of the substrate-free ASST-(His436Asn) against crystallographic data from the soaking experiments using Refmac.[24] Further refinement, including the occupancy of the sulfuryl donor, was performed using Phenix[25] and Coot.[23] All X-ray data collection, phasing, and refinement statistics are presented in Table 1. Figures were prepared using Pymol.[27]

Fluorimetric Titration. Fluorescence titration of ASST-(Cys322Ala) with MUS was performed in 20 mM Tris/HCl at pH 8.0, 400 mM NaCl, and 1 mM EDTA by adding aliquots of ASST (20 μL, 20 μM) into a 2 mL solution of MUS (1.7 μM) and monitoring the MU formation signal for 60 s (data interval 1 s) on a Photon Technology International fluorimeter at (25 ± 0.2) °C in a fluorescence cuvette (10 × 10 mm) with magnetic stirring. An excitation wavelength of (350 ± 2.5) nm was used, and emission was recorded at (453 ± 2.5) nm. Fluorescence intensities were averaged and corrected for dilution.

Kinetics of ASST sulfurylation. The kinetics of ASST-(Cys322Ala) sulfurylation by MUS was monitored by a change of fluorescence at 453 nm (excitation wavelength was 350 nm) at (25 ± 0.2) °C in a 1:1 volume mixing ratio in 20 mM Tris/HCl at pH 8.0, 400 mM NaCl, and 1 mM EDTA. Measurements were performed under pseudo-first-order conditions with an initial protein concentration of 1 μM and MUS at 9.54 μM in a stopped flow apparatus (Applied Photophysics SX-17MV). Desulfo-ASST was prepared by incubating ASST with phenol for 2 h at 25 °C, and phenol was removed by multiple cycles of ultrafiltration (Amicon YM10, Millipore) in the same buffer. Fluorescence data from nine independent measurements were fitted individually according to the formula $F = F_\infty + (F_0 - F_\infty) \times \exp(-t \times {}^2k \times [\mathrm{MUS}])$, where F is the fluorescence intensity, F_∞ and F_0 are the fluorescence signals at the end and the beginning of the reaction, respectively, t is the reaction time, ${}^2k$ is the second order rate constant, and [MUS] is the concentration of MUS at the beginning of reaction and the mean value of ${}^2k$ plus/minus its standard deviation from the nine measurements reported.

Analysis of ASST Sulfurylation by Human Urine. ASST was incubated with 2 mM phenol for 2 h at 25 °C to prepare the desulfurylated protein, and phenol was removed by multiple cycles of ultrafiltration in 20 mM Tris/HCl at pH 8.0 and 1 mM EDTA (Amicon YM10, Millipore). Such an ASST preparation was mixed with an equal volume of either the same buffer, PNS (300 μM), or human urine and analyzed by electrospray ionization mass spectrometry. The urine was collected from a healthy 28-year-old male donor, who exhibited no clinical symptoms of urinary tract infection, was on no medications, and had no history of renal dysfunction. The resulting mass spectra of ASST were normalized so that the strongest peak (desulfo-ASST) corresponds to 100% intensity. Identical results were obtained from the experiment performed in triplicate with urine samples collected on different days and following different meals.

ESI-MS. Electrospray ionization mass spectrometry was performed at the Functional Genomics Center Zurich (FGCZ) using standard techniques. Protein samples were desalted using ZipTips (Millipore) and analyzed in 50% acetonitrile/0.2% formic acid (pH 2).

Kinetics of Disulfide Bond Introduction. DsbA, DsbL, and the peptide comprising the residues 411−429 of ASST (Ac-ANGKPITCNENGLCENSDF-$CONH_2$) (Genscript, USA) was dissolved in degassed and sterile filtered 20 mM phosphoric acid/NaOH at pH 7.0, 100 mM NaCl, and 0.1 mM EDTA to 2 μM. Stopped flow fluorescence measurements were performed at 25 ± 0.2 °C, with excitation at 280 nm and recording the emission above 320 nm. The reactants were mixed in a 1:1 ratio, yielding identical initial concentrations of 1 μM for all reactants. Fluorescence kinetics were fitted to a second-order mechanism with Sigmaplot.

RESULTS AND DISCUSSION

Structure of the Trapped Catalytic Intermediates of ASST. In order to capture the presulfurylation state of ASST, we sought to replace the active site residue histidine-436 by one that cannot undergo sulfurylation but is otherwise similar in size and properties to histidine. On the basis of these criteria, we selected asparagine, and the resulting variant (ASST His436Asn) crystallized under the same conditions as the wild-type protein[17] and exhibited identical structure in the apo-state as well as upon soaking with PNS or MUS (RMSD of C_α atoms 0.26 Å) (Figure 1).

As opposed to the structure of the wild-type protein, where a sulfate ion is found in close proximity to the catalytic residue His436,[17] a molecule of 3-(*N*-morpholino)propanesulfonic acid (MOPS), the compound used as a buffer for ASST purification, was found in the active site of the His436Asn variant of ASST (Figure 1A). Its sulfonic acid moiety was found to make an extensive hydrogen bond network with the nearby His252, His356, Asn358, Arg374, Asn436, and the backbone nitrogen of Thr501. It is likely that a MOPS molecule is able to bind to the active site of this mutant, but not wild-type protein due to the smaller size of Asn vs His side chains, which allows for more extensive interactions of Phe171 and Ile500 with this ligand. Upon soaking of crystals of this protein variant with PNS or MUS, the sulfuryl donor substrates bound to the active site, but did not sulfurylate the mutant protein, providing structural insight into the presulfurylation state. PNS (Figure 1B) and MUS (Figure 1C) were found to bind to the active site of the ASST His436Asn with the aromatic rings oriented like those of the products 4-nitrophenol (PN) and 4-methylumbelliferone (MU) in the trapped postsulfurylation state.[17] Aryl sulfates are bound to the enzyme active site by a network of hydrogen bonds from the side chains of His252, His356, Asn358, Arg374, Asn436, and Thr501, as well as the hydrophobic interactions between Phe171 and Ile500 and their aromatic rings.

Structural superposition of postsulfurylation wild-type ASST in complex with PN and presulfurylation ASST His436Asn mutant with PNS reveals a nearly identical active site geometry, where both the polar sulfuryl groups and the apolar aromatic moieties occupy identical positions (Figure 2). This spatial arrangement enables the same network of hydrogen bonds between the sulfate group and nitrogens from active site residues as well as the two hydrophobic side chains and the

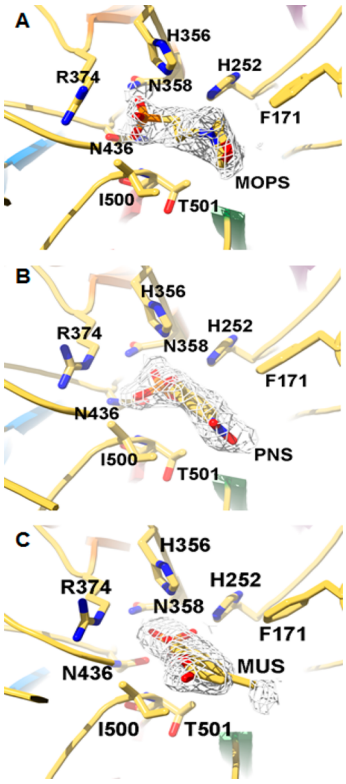

Figure 1. Active site of (A) apo-ASST-His436Asn (containing an ordered molecule of the buffer 3-(*N*-morpholino)propanesulfonic acid in the active site) and its complex with the aromatic sulfuryl donor compounds (B) PNS and (C) MUS. The residues interacting with substrates are indicated. Omit maps are shown as gray mesh around the ligands and contoured at 1σ. The blades of the β-propeller are colored individually using the same color scheme as in previous publications on ASST[17,6] with blades 1 through 6 in red, green, cyan, pink, orange, and blue, respectively. This color scheme is used consistently throughout this article. A stereo version of this figure is provided as Supporting Information.

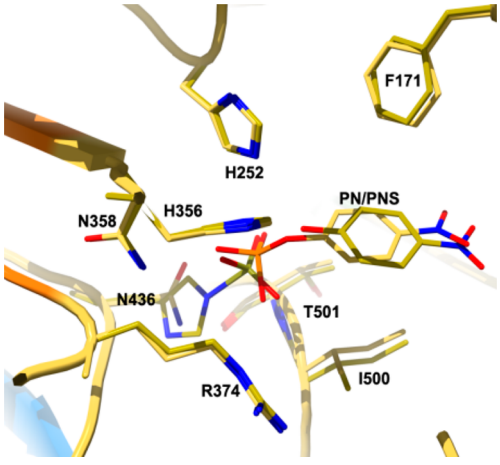

Figure 2. Overlay of PNS-bound His436Asn ASST structure with the wild-type sulfo-ASST in complex with PN. Active site residues and the ligands are shown in stick format.

aromatic rings (Figure 2)[17] and suggests that physiological donor and acceptor substrates are likely chemically very similar, at least in their segment that binds to the active site of ASST. Furthermore, it implies that the two half-reactions of the ASST catalytic cycle are a reverse of each other. A recent comparison of the structure of the sulfo-ASST in complex with PN[17] with the active site of an unrelated mouse ST (mSULT1D1)[28] suggested that the sulfotransfer reaction proceeds through an "S_N2-like" mechanism in both proteins.[29] The observation of a similar arrangement in this presulfurylation state provides additional support for this claim.

To test whether all active sites of ASST participate in catalysis and act independently, the sulfuryl donor MUS was titrated with increasing amounts of desulfurylated ASST. Figure 3 shows that the sulfurylation of ASST consumes one molecule

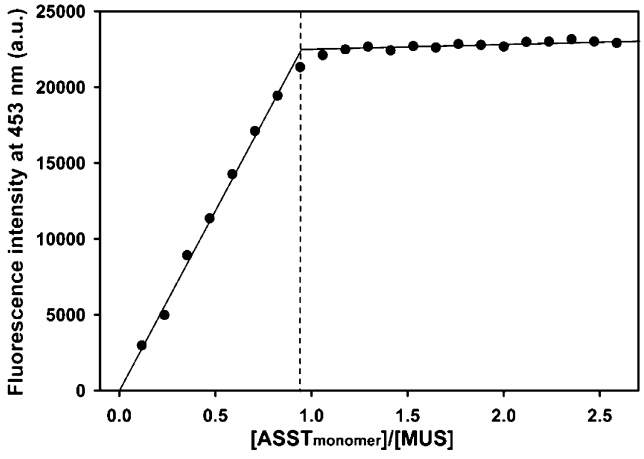

Figure 3. Titration of MUS with ASST at pH 8.0 and 25 °C reveals a 1:1 stoichiometry for the sulfurylation of each active site by MUS. ASST aliquots were added to MUS (1.7 μM) stepwise, and the resulting enzyme sulfurylation was monitored fluorimetrically via the specific fluorescence of the reaction product MU. Linear fits of data before and after the point of equivalence (solid lines) suggest a molar ratio of ASST monomers to MUS of (0.93 ± 0.03) at the equivalence (dashed line).

of sulfuryl donor per ASST monomer; thus, both active sites of the homodimer can be sulfurylated and participate in catalysis simultaneously. This observation is in agreement with the crystallographic data, which reveal ligands in both active sites.

The physiological substrates of ASST in *E. coli* CFT073 have not been identified. Given that sulfurylated compounds are implicated in extracellular communication, and particularly host-pathogen interactions, and that *E. coli* ASST is upregulated during urinary tract infection,[9] it is possible that human urine contains ASST substrates. To test this hypothesis, we incubated desulfo-ASST with human urine. Mass spectrometry (Figure 4A) revealed enzyme sulfurylation, confirming that sulfuryl donors for ASST are indeed present in human urine. In order to identify these substrates crystallographically, any sulfuryl groups remaining after purification were removed by treating ASST with phenol prior to crystallization.[17] ASST crystals were then soaked with human urine: this caused significant damage to crystals, most readily observed through a degradation in the diffracting power with a concomitant decrease in the resolution of data that could be collected (2.59 Å). Nonetheless, positive electron density was clearly observed in the active site indicating a bound ligand. The resolution of the diffraction data did not allow unambiguous identification of the ligand, but this observation provides additional confirmation that human urine contains ASST substrates. Ambiguity in the identity of the substrate may also arise from the fact that ASST molecules

dx.doi.org/10.1021/bi401725j | *Biochemistry* 2014, 53, 1870−1877

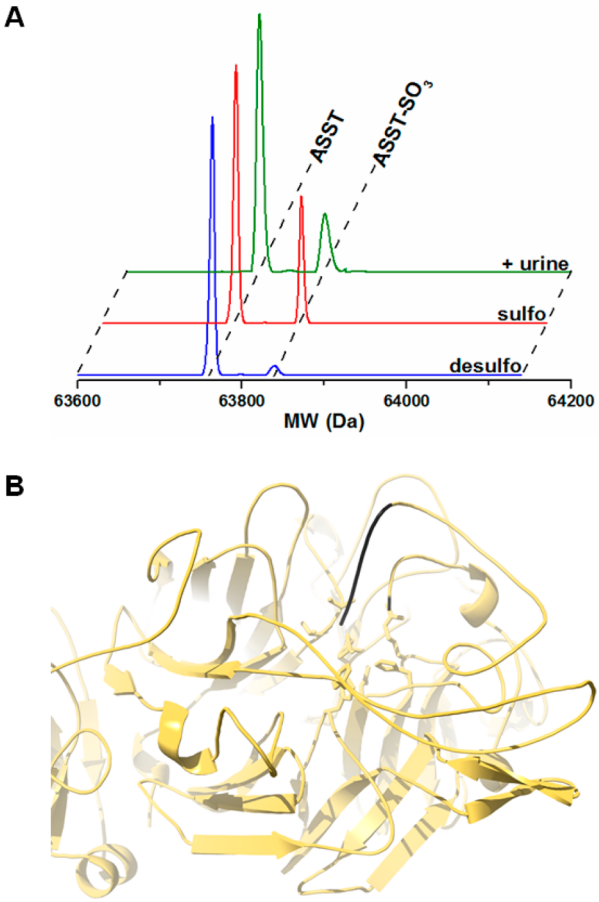

Figure 4. (A) Sulfurylation of ASST by human urine monitored by electrospray ionization mass spectrometry. ASST treated by phenol (blue) exhibits the mass of 63764.5 Da as expected for its amino acid composition. Incubation of desulfo-ASST with PNS results in a fraction (about one-third) of the protein exhibiting 80 Da higher mass (addition of the SO_3^- group to the protein, red). This peak is also observed when desulfo-ASST is treated with urine (green). Mass spectra never reveal complete sulfurylation of ASST most likely due to a limited stability of sulfohistidine against hydrolysis under the applied conditions.[17] (B) In the structure of urine-soaked ASST, the ASST loop consisting of residues 321−328 (but still lacking the residue 322) can be clearly observed and extends toward the active site (the segment of the loop that became ordered is highlighted in black).

bound several different sulfophenolic compounds, each of which occupy a fraction of the active sites, and their superposition results in uninterpretable ligand electron density.

In the ASST structures elucidated so far, readily interpretable electron density is present for all residues of this protein, except for the loop just above the active site, consisting of residues 321−327, which is presumably disordered. However, upon soaking with urine, this disordered loop became clearly visible and extends directly into the active site. In this position, it would sterically clash with a bound phenolic substrate (Figure 4B). It is possible that this loop exists in two states, a disordered one and a highly ordered one, covering the active site, and the treatment with urine captures it in the ordered one.

Microscopic rate constants for the individual steps of the ASST reaction cycle are unknown. To characterize the kinetics of ASST sulfurylation with model substrates, we measured the rate of ASST sulfurylation by MUS using stopped-flow mixing under pseudo-first-order conditions (Figure 5). The reaction exhibited a single phase corresponding to enzyme sulfurylation

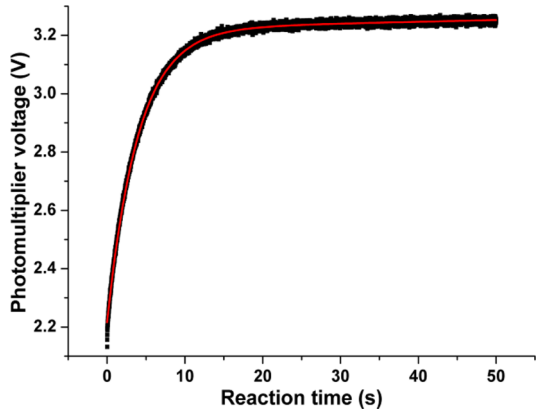

Figure 5. Representative measurement of kinetics of ASST sulfurylation by MUS at pH 8.0 and 25 °C, monitored by the increase in the fluorescence of the product MU. Data from nine independent measurements were fitted individually according to pseudo-first-order kinetics (solid red line; initial concentrations, 9.54 μM MUS and 1 μM ASST).

with a second-order rate constant of $^2k = (2.51 \pm 0.03) \times 10^4$ $M^{-1}s^{-1}$. The observations that ASST sulfurylation follows single-exponential kinetics and that both ASST monomers can bind MUS simultaneously demonstrate that active sites in the ASST dimers are independent.

The half-life for ASST sulfurylation by MUS under the conditions in Figure 5 is roughly 2 s. Given that the reaction was performed with an initial protein concentration of 1 μM and MUS at 9.54 μM, at saturating, 100-fold higher MUS concentration (954 μM, around 20 times its K_M value ($K_{M,MUS} = (4.45 \pm 0.72) \times 10^{-5}$ M)[17]), the half-life of this reaction is expected to be about 20 ms. This value is in excellent agreement with the time required for single turnover calculated as the reciprocal value of k_{cat} at saturating substrate concentrations obtained from Michaelis−Menten measurements ($k_{cat} = (48.6 \pm 0.5)$ s^{-1}),[17] which equates to 20.6 ms. Therefore, under the experimental conditions, enzyme sulfurylation by the donor (first half-reaction) is rate limiting for ASST catalysis or equally fast as acceptor substrate sulfurylation (second half-reaction). However, the actual rate limiting step for ASST catalysis will depend on the concentrations of donor and acceptor substrate compounds *in vivo* and their respective K_M values.

Kinetics of Disulfide Bond Formation in ASST by DsbL and DsbI. The structural disulfide bond Cys418-Cys424 is buried in the ASST structure and thus needs to be introduced by periplasmic dithiol oxidases prior to ASST folding. To determine the rate of formation of the Cys418-Cys424 disulfide bond in unfolded ASST by the oxidized form of DsbL and DsbA, the kinetics of the dithiol/disulfide exchange between each of these oxidoreductases and the unstructured model peptide ANGKPITCNENGLCENSDF comprising ASST residues 411−429 (with Cys418 and Cys424) was measured via the increase in enzyme fluorescence upon reduction (Figure 6). The data revealed that disulfide bond formation in the peptide occurred with a rate constant of $^2k_{DsbL} = (9.62 \pm 0.04) \times 10^4$ $M^{-1}s^{-1}$ and $^2k_{DsbA} = (4.94 \pm 0.01) \times 10^5$ $M^{-1}s^{-1}$ for DsbL and DsbA, respectively.

dx.doi.org/10.1021/bi401725j | *Biochemistry* 2014, 53, 1870−1877

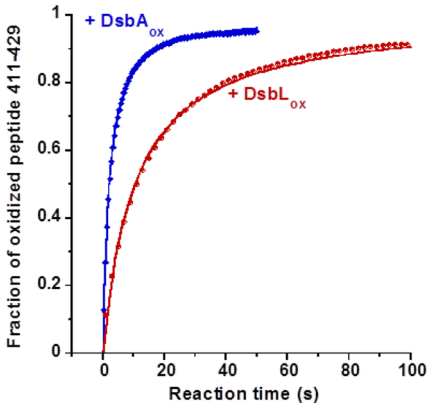

Figure 6. Kinetics of dithiol/disulfide exchange reaction between oxidized DsbA (blue rhombi) or oxidized DsbL (red circles) and the reduced peptide corresponding to ASST residues 411−429 at pH 7.0 and 25 °C (initial concentrations of all reactants were 1.0 μM). The reactions were followed via the increase in tryptophan fluorescence of DsbA or DsbL upon reduction, evaluated according to second-order kinetics (solid lines) and normalized. The ASST peptide 411−429 lacks tyrosines and tryptophans and is spectroscopically silent in both reactions.

The fact that the disulfide bond in ASST is formed even 5 times faster with DsbA compared to DsbL suggests that an ASST-specific chaperone effect of DsbL, which is not present in DsbA, is critical for the dependence on DsbL of efficient ASST folding *in vivo*.[19]

CONCLUSIONS

In summary, the crystallographic work described here provides the structural snapshot of the presulfurylation state of an ASST with substrates in the active site. It reveals the similarities of donor and acceptor substrate recognition, common among enzymes that follow the ping−pong bi−bi kinetic mechanism to transfer moieties among chemically similar entities.[30] Intriguingly, the structures demonstrate that the sulfuryl group of the donor and the acceptor atoms are positioned exactly like those in the structure of a PAPS-dependent ST.[28,29,31] This pronounced similarity of spatial arrangements in the active site, despite the completely different folds and kinetic mechanisms of these two classes of STs,[1] underscores the conserved chemistry of sulfotransfer catalysis. Furthermore, it supports the notion that the two different classes of STs have evolutionarily converged to catalyze the same reaction.[9] Although the homooligomeric state of ASST could allow for allosteric effects,[30] our kinetic and thermodynamic data revealed that both active sites of ASST are independent.

ASST is present in bacterial pathogens; among *E. coli*, it is found only in uropathogenic strains and upregulated during urinary tract infection.[9] Even though ASST-like proteins were recently reported to play a role in the biosynthesis of liponucleoside antibiotics in *Streptomycetes*,[10−13] the function of *E. coli* CFT073 ASST and its potential involvement in urinary tract infection remain elusive. Unlike the communication inside the cell, which usually involves a cascade of phosphorylation reactions, extracellular communication and host−pathogen interactions are frequently mediated by sulfurylated small molecules.[32,33] The periplasmic location of ASST and its ability to catalyze sulfotransfer between small phenolic compounds suggest its natural substrates may be present in human urine, known to contain sulfurylated metabolites.[34] Our structural and mass spectrometric experiments demonstrated that ASST indeed reacts with donor(s) from human urine. Even though the urine incubation experiment has not been performed in a statistically significant manner, it is attractive to speculate that the physiological sulfuryl donor compounds stem from the host organism, while the physiological acceptor substrates might originate from bacterial cells since ASST was found sulfurylated (but not desulfurylated) upon incubation with human urine. However, an identification of natural substrates of ASST is eagerly awaited to shed light on the role of small sulfurylated phenols in host−pathogen ineractions. Along with the structures of ASST presented herein and previously,[17] the information on binding of these compounds to the active site of ASST will be helpful to guide structure-based drug design targeting ASST.

The genes for the generic periplasmic dithiol oxidase DsbA, which introduces disulfide bonds into the folding envelope and secretory proteins, and its oxidase from the inner bacterial membrane DsbB, which generates disulfides *de novo* by reducing quinones, are distant from each other on the *E. coli* genome. However, the *assT* gene is always found clustered in the same operon with the gene for *dsbL* and often *dsbI* as well, which encode paralogues of DsbA and DsbB, respectively.[6,19] The genes for a protein are commonly found clustered with those helping their folding,[35] which is especially true for large, topologically complex proteins.[36] Accordingly, it has been demonstrated that the levels of ASST depend on the functional DsbL/DsbI redox couple even in the presence of DsbA and DsbB.[19] Our results reveal that both DsbA and DsbL are able to introduce the disulfide bond into the model ASST peptide at similar rates. If the rate limiting step of ASST folding were the formation of the disulfide bond, the rates of folding would be expected to reflect the rates of disulfide bond formation. Since this is not the case, a chaperone effect of DsbL, not present in DsbA, is likely to be critical for the folding of ASST and not its oxidase activity. Interestingly, the disulfide bond in ASST is highly conserved, and its stereochemical parameters suggest that it belongs to the highly strained −RHStaple category.[17,37] Such disulfide bonds are frequently found to regulate protein function by forming or breaking in the mature protein and are termed allosteric disulfides.[38,39] Since this disulfide is located close to the surface of the protein and is in the same blade (6) of the β-propeller, just 12 residues ahead of the catalytic residue His436, it will be interesting to address whether such allosteric control is happening and under which circumstances.

ASSOCIATED CONTENT

Supporting Information

A stereo view of the active site of apo-ASST-His436Asn (containing an ordered molecule of the buffer 3-(*N*-morpholino)propanesulfonic acid in the active site) and its complex with the aromatic sulfuryl donor compounds PNS and MUS. This material is available free of charge via the Internet at http://pubs.acs.org.

Accession Codes

The atomic coordinates of desulfo-ASST His436Asn and its complexes with PNS, MUS, and the complex of wild-type ASST with human urine have been deposited in the Protein Data Bank, www.pdb.org under the accession codes reported in Table 1.

AUTHOR INFORMATION

Corresponding Author

*ETH Zurich, Institute of Molecular Biology and Biophysics, HPK E14, CH-8093 Zurich, Switzerland. Phone: 41-44-633-6819. Fax: 41-44-633-1036. E-mail: malojcic@fas.harvard.edu; goran.malojcic@alumni.ethz.ch.

Present Address

(G.M.) Harvard University, Department of Chemistry and Chemical Biology, 12 Oxford Street, Cambridge, MA, 02138, USA.

Funding

This work was supported by the Swiss Light Source (Paul Scherrer Institut, Villigen, Switzerland), Swiss National Science Foundation, and ETH Zurich in the framework of the NCCR Structural Biology program. G.M. is currently supported by the Advanced Postdoc Mobility Fellowship by the Swiss National Science Foundation.

Notes

The authors declare no competing financial interest.

ACKNOWLEDGMENTS

We are grateful to C. Schulze-Briese for advice and assistance with experiments at the protein crystallography beam lines of the SLS, S. Chesnov of the FGCZ for protein analytics services, and Hiang Dreher-Teo for technical assistance.

REFERENCES

(1) Chapman, E., Best, M. D., Hanson, S. R., and Wong, C. H. (2004) Sulfotransferases: structure, mechanism, biological activity, inhibition, and synthetic utility. *Angew. Chem., Int. Ed. 43*, 3526−3548.

(2) Kim, D. H., Kim, H. S., and Kobashi, K. (1992) Purification and characterization of novel sulfotransferase obtained from Klebsiella K-36, an intestinal bacterium of rat. *J. Biochem. 112*, 456−460.

(3) Kim, D. H., and Kobashi, K. (1991) Kinetic studies on a novel sulfotransferase from Eubacterium A-44, a human intestinal bacterium. *J. Biochem. 109*, 45−48.

(4) Kwon, A. R., Yun, H. J., and Choi, E. C. (2001) Kinetic mechanism and identification of the active site tyrosine residue in *Enterobacter amnigenus* arylsulfate sulfotransferase. *Biochem. Biophys. Res. Commun. 285*, 526−529.

(5) Lee, N. S., Kim, B. T., Kim, D. H., and Kobashi, K. (1995) Purification and reaction mechanism of arylsulfate sulfotransferase from Haemophilus K-12, a mouse intestinal bacterium. *J. Biochem. 118*, 796−801.

(6) Malojcic, G., and Glockshuber, R. (2010) The PAPS-independent aryl sulfotransferase and the alternative disulfide bond formation system in pathogenic bacteria. *Antioxid. Redox Signaling 13*, 1247−1259.

(7) Lawley, T. D., Chan, K., Thompson, L. J., Kim, C. C., Govoni, G. R., and Monack, D. M. (2006) Genome-wide screen for Salmonella genes required for long-term systemic infection of the mouse. *PLoS Pathog. 2*, e11.

(8) Mathew, J. A., Tan, Y. P., Srinivasa Rao, P. S., Lim, T. M., and Leung, K. Y. (2001) *Edwardsiella tarda* mutants defective in siderophore production, motility, serum resistance and catalase activity. *Microbiology 147*, 449−457.

(9) Lloyd, A. L., Rasko, D. A., and Mobley, H. L. (2007) Defining genomic islands and uropathogen-specific genes in uropathogenic *Escherichia coli*. *J. Bacteriol. 189*, 3532−3546.

(10) Funabashi, M., Baba, S., Nonaka, K., Hosobuchi, M., Fujita, Y., Shibata, T., and Van Lanen, S. G. (2010) The biosynthesis of liposidomycin-like A-90289 antibiotics featuring a new type of sulfotransferase. *ChemBioChem 11*, 184−190.

(11) Kaysser, L., Eitel, K., Tanino, T., Siebenberg, S., Matsuda, A., Ichikawa, S., and Gust, B. (2010) A new arylsulfate sulfotransferase involved in liponucleoside antibiotic biosynthesis in streptomycetes. *J. Biol. Chem. 285*, 12684−12694.

(12) Tang, X., Eitel, K., Kaysser, L., Kulik, A., Grond, S., and Gust, B. (2013) A two-step sulfation in antibiotic biosynthesis requires a type III polyketide synthase. *Nat. Chem. Biol. 9*, 610−615.

(13) Van Lanen, S. G. (2013) Biosynthesis: a sulfonate relay revealed. *Nat. Chem. Biol. 9*, 602−603.

(14) Kobashi, K., Fukaya, Y., Kim, D. H., Akao, T., and Takebe, S. (1986) A novel type of aryl sulfotransferase obtained from an anaerobic bacterium of human intestine. *Arch. Biochem. Biophys. 245*, 537−539.

(15) van der Horst, M. A., van Lieshout, J. F. T., Bury, A., Hartog, A. F., and Wever, R. (2012) Sulfation of various alcoholic groups by an arylsulfate sulfotransferase from desulfitobacterium hafniense and synthesis of estradiol sulfate. *Adv. Synth. Catal. 354*, 3501−3508.

(16) Welch, R. A., Burland, V., Plunkett, G., 3rd, Redford, P., Roesch, P., Rasko, D., Buckles, E. L., Liou, S. R., Boutin, A., Hackett, J., Stroud, D., Mayhew, G. F., Rose, D. J., Zhou, S., Schwartz, D. C., Perna, N. T., Mobley, H. L., Donnenberg, M. S., and Blattner, F. R. (2002) Extensive mosaic structure revealed by the complete genome sequence of uropathogenic *Escherichia coli*. *Proc. Natl. Acad. Sci. U.S.A. 99*, 17020−17024.

(17) Malojcic, G., Owen, R. L., Grimshaw, J. P., Brozzo, M. S., Dreher-Teo, H., and Glockshuber, R. (2008) A structural and biochemical basis for PAPS-independent sulfuryl transfer by aryl sulfotransferase from uropathogenic *Escherichia coli*. *Proc. Natl. Acad. Sci. U.S.A. 105*, 19217−19222.

(18) Sun, M., and Leyh, T. S. (2010) The human estrogen sulfotransferase: a half-site reactive enzyme. *Biochemistry 49*, 4779−4785.

(19) Grimshaw, J. P., Stirnimann, C. U., Brozzo, M. S., Malojcic, G., Grutter, M. G., Capitani, G., and Glockshuber, R. (2008) DsbL and DsbI form a specific dithiol oxidase system for periplasmic arylsulfate sulfotransferase in uropathogenic *Escherichia coli*. *J. Mol. Biol. 380*, 667−680.

(20) Kabsch, W. (2010) Xds. *Acta Crystallogr., Sect. D 66*, 125−132.

(21) Evans, P. (1993) Data Reduction, in *CCP4 Daresbury Study Weekend*, pp 114−122, Daresbury Laboratory, Warrington, U.K.

(22) McCoy, A. J., Grosse-Kunstleve, R. W., Storoni, L. C., and Read, R. J. (2005) Likelihood-enhanced fast translation functions. *Acta Crystallogr., Sect. D 61*, 458−464.

(23) Emsley, P., and Cowtan, K. (2004) Coot: model-building tools for molecular graphics. *Acta Crystallogr., Sect. D 60*, 2126−2132.

(24) Murshudov, G. N., Vagin, A. A., Lebedev, A., Wilson, K. S., and Dodson, E. J. (1999) Efficient anisotropic refinement of macromolecular structures using FFT. *Acta Crystallogr., Sect. D 55*, 247−255.

(25) Adams, P. D., Grosse-Kunstleve, R. W., Hung, L. W., Ioerger, T. R., McCoy, A. J., Moriarty, N. W., Read, R. J., Sacchettini, J. C., Sauter, N. K., and Terwilliger, T. C. (2002) PHENIX: building new software for automated crystallographic structure determination. *Acta Crystallogr., Sect. D 58*, 1948−1954.

(26) Chen, V. B., Arendall, W. B., III, Headd, J. J., Keedy, D. A., Immormino, R. M., Kapral, G. J., Murray, L. W., Richardson, J. S., and Richardson, D. C. (2010) MolProbity: all-atom structure validation for macromolecular crystallography. *Acta Crystallogr., Sect. D 66*, 12−21.

(27) DeLano, W. L. (2002) *The PyMOL Users Manual*, DeLano Scientific, Palo Alto, CA.

(28) Teramoto, T., Adachi, R., Sakakibara, Y., Liu, M. C., Suiko, M., Kimura, M., and Kakuta, Y. (2009) On the similar spatial arrangement of active site residues in PAPS-dependent and phenolic sulfate-utilizing sulfotransferases. *FEBS Lett. 583*, 3091−3094.

(29) Teramoto, T., Sakakibara, Y., Liu, M. C., Suiko, M., Kimura, M., and Kakuta, Y. (2009) Snapshot of a Michaelis complex in a sulfuryl transfer reaction: Crystal structure of a mouse sulfotransferase, mSULT1D1, complexed with donor substrate and accepter substrate. *Biochem. Biophys. Res. Commun. 383*, 83−87.

(30) Cook, P. F., and Cleland, W. W. (2007) *Enzyme Kinetics and Mechanism*, Garland, New York.

(31) Teramoto, T., Sakakibara, Y., Liu, M. C., Suiko, M., Kimura, M., and Kakuta, Y. (2009) Structural basis for the broad range substrate specificity of a novel mouse cytosolic sulfotransferase–mSULT1D1. *Biochem. Biophys. Res. Commun. 379*, 76−80.
(32) Bowman, K. G., and Bertozzi, C. R. (1999) Carbohydrate sulfotransferases: mediators of extracellular communication. *Chem. Biol. 6*, R9−R22.
(33) Pi, N., Yu, Y., Mougous, J. D., and Leary, J. A. (2004) Observation of a hybrid random ping-pong mechanism of catalysis for NodST: a mass spectrometry approach. *Protein Sci. 13*, 903−912.
(34) Manach, C., Scalbert, A., Morand, C., Remesy, C., and Jimenez, L. (2004) Polyphenols: food sources and bioavailability. *Am. J. Clin. Nutr. 79*, 727−747.
(35) Rodriguez-Pena, J. M., Alvarez, I., Ibanez, M., and Rotger, R. (1997) Homologous regions of the *Salmonella enteritidis* virulence plasmid and the chromosome of *Salmonella typhi* encode thiol: disulphide oxidoreductases belonging to the DsbA thioredoxin family. *Microbiology 143* (Pt 4), 1405−1413.
(36) Vertommen, D., Ruiz, N., Leverrier, P., Silhavy, T. J., and Collet, J. F. (2009) Characterization of the role of the *Escherichia coli* periplasmic chaperone SurA using differential proteomics. *Proteomics 9*, 2432−2443.
(37) Schmidt, B., Ho, L., and Hogg, P. J. (2006) Allosteric disulfide bonds. *Biochemistry 45*, 7429−7433.
(38) Azimi, I., Wong, J. W., and Hogg, P. J. (2011) Control of mature protein function by allosteric disulfide bonds. *Antioxid. Redox Signaling 14*, 113−126.
(39) Cook, K. M., and Hogg, P. J. (2013) Post-translational control of protein function by disulfide bond cleavage. *Antioxid. Redox Signaling 18*, 1987−2015.